Received: 2 November 2018 | Revised: 10 March 2019 | Accepted: 10 April 2019

DOI: 10.1111/geb.12933

RESEARCH PAPER

Global Ecology and Biogeography A Journal of Macroecology WILEY

Spatio-temporal patterns of tree growth as related to carbon isotope fractionation in European forests under changing climate

Tatiana A. Shestakova[1] | Jordi Voltas[2] | Matthias Saurer[3] | Frank Berninger[4] | Jan Esper[5] | Laia Andreu-Hayles[6] | Valérie Daux[7] | Gerhard Helle[8] | Markus Leuenberger[9] | Neil J. Loader[10] | Valérie Masson-Delmotte[7] | Antonio Saracino[11] | John S. Waterhouse[12] | Gerhard H. Schleser[13] | Zdzisław Bednarz[14] | Tatjana Boettger[15] | Isabel Dorado-Liñán[16] | Marc Filot[9] | David Frank[17] | Michael Grabner[18] | Marika Haupt[15] | Emmi Hilasvuori[19] | Högne Jungner[19] | Maarit Kalela-Brundin[20] | Marek Krąpiec[21] | Hamid Marah[22] | Sławomira Pawełczyk[23] | Anna Pazdur[23] | Monique Pierre[7] | Octavi Planells[24] | Rūtilė Pukienė[25] | Christina E. Reynolds-Henne[26] | Katja T. Rinne-Garmston (Rinne)[27] | Angelo Rita[28] | Eloni Sonninen[19] | Michel Stiévenard[7] | Vincent R. Switsur[12†] | Elżbieta Szychowska-Krąpiec[21] | Malgorzata Szymaszek[23] | Luigi Todaro[28] | Kerstin Treydte[3] | Adomas Vitas[29] | Martin Weigl[30] | Rupert Wimmer[31] | Emilia Gutiérrez[24]

[1]Woods Hole Research Center, Falmouth, Massachusetts

[2]Department of Crop and Forest Sciences – AGROTECNIO Center, University of Lleida, Lleida, Spain

[3]Swiss Federal Research Institute WSL, Birmensdorf, Switzerland

[4]Department of Forest Sciences, University of Helsinki, Helsinki, Finland

[5]Department of Geography, Johannes Gutenberg University, Mainz, Germany

[6]Tree-Ring Laboratory, Lamont–Doherty Earth Observatory of Columbia University, Palisades, New York

[7]Laboratory for Climate and Environmental Sciences, CEA/CNRS, UVSQ, Gif-sur-Yvette, France

[8]Helmholtz-Centre Potsdam, German Centre for Geosciences – GFZ, Potsdam, Germany

[9]Climate and Environmental Physics, University of Bern, Bern, Switzerland

[10]Department of Geography, Swansea University, Swansea, UK

[11]Department of Agricultural Sciences, University of Naples Federico II, Portici, Italy

[12]Department of Biomedical and Forensic Sciences, Anglia Ruskin University, Cambridge, UK

[13]FZJ Research Center Jülich, Institute of Bio- and Geosciences IBG-3, Jülich, Germany

[14]Department of Forest Biodiversity, Agricultural University, Krakow, Poland

[15]Department of Isotope Hydrology, Helmholtz Centre for Environmental Research – UFZ, Halle, Germany

[16]Forest Research Centre, National Institute for Agricultural Research and Experimentation (INIA-CIFOR), Madrid, Spain

[17]Laboratory of Tree-Ring Research, University of Arizona, Tucson, Arizona

[18]Institute of Wood Technology and Renewable Resources, University of Natural Resources and Life Sciences – BOKU, Vienna, Austria

[19]Laboratory of Chronology, University of Helsinki, Helsinki, Finland

[†]Deceased

[20]Forestry Museum, Lycksele, Sweden
[21]Faculty of Geology, Geophysics and Environmental Protection, AGH University of Science and Technology, Krakow, Poland
[22]Water and Climate Unit, CNESTEN, Rabat, Morocco
[23]Department of Radioisotopes, Silesian University of Technology, Gliwice, Poland
[24]Department of Biological Evolution, Ecology and Environmental Sciences, University of Barcelona, Barcelona, Spain
[25]The State Scientific Research Institute Nature Research Centre, Vilnius, Lithuania
[26]Oeschger Centre for Climate Change Research, University of Bern, Bern, Switzerland
[27]Natural Resources Institute Finland (Luke), Helsinki, Finland
[28]School of Agricultural, Forest, Food and Environmental Sciences, University of Basilicata, Potenza, Italy
[29]Environmental Research Centre, Vytautas Magnus University, Kaunas, Lithuania
[30]Holzforschung Austria, Vienna, Austria
[31]Institute for Natural Materials Technology, University of Natural Resources and Life Sciences, Tulln, Austria

Correspondence
Emilia Gutiérrez, Department of Evolutionary Biology, Ecology and Environmental Sciences, University of Barcelona, Avda. Diagonal 643, Barcelona 08028, Spain
Email: emgutierrez@ub.edu

Present Address
Marc Filot, CSL Behring AG, Bern, Switzerland

Malgorzata Szymaszek, Janusz Kusocinski Sports School in Zabrze, Zabrze, Poland

Funding information
Spanish Government, Grant/Award Number: AGL2015-68274-C3-3-R; Sixth Framework Programme, Grant/Award Number: EVK2-2001-00237; Seventh Framework Programme, Grant/Award Number: COST-STSM-ECOST-STSM-FP1304-140915-066395 and ERANET-Mundus program (Grant agreement 20112573)

Editor: Thomas Hickler

Abstract

Aim: The aim was to decipher Europe-wide spatio-temporal patterns of forest growth dynamics and their associations with carbon isotope fractionation processes inferred from tree rings as modulated by climate warming.

Location: Europe and North Africa (30–70° N, 10° W–35° E).

Time period: 1901–2003.

Major taxa studied: Temperate and Euro-Siberian trees.

Methods: We characterize changes in the relationship between tree growth and carbon isotope fractionation over the 20th century using a European network consisting of 20 site chronologies. Using indexed tree-ring widths (TRW_i), we assess shifts in the temporal coherence of radial growth across sites (synchrony) for five forest ecosystems (Atlantic, boreal, cold continental, Mediterranean and temperate). We also examine whether TRW_i shows variable coupling with leaf-level gas exchange, inferred from indexed carbon isotope discrimination of tree-ring cellulose ($\Delta^{13}C_i$).

Results: We find spatial autocorrelation for TRW_i and $\Delta^{13}C_i$ extending over a maximum of 1,000 km among forest stands. However, growth synchrony is not uniform across Europe, but increases along a latitudinal gradient concurrent with decreasing temperature and evapotranspiration. Latitudinal relationships between TRW_i and $\Delta^{13}C_i$ (changing from negative to positive southwards) point to drought impairing carbon uptake via stomatal regulation for water saving occurring at forests below 60° N in continental Europe. An increase in forest growth synchrony over the 20th century together with increasingly positive relationships between TRW_i and $\Delta^{13}C_i$ indicate intensifying impacts of drought on tree performance. These effects are noticeable in drought-prone biomes (Mediterranean, temperate and cold continental).

Main conclusions: At the turn of this century, convergence in growth synchrony across European forest ecosystems is coupled with coordinated warming-induced effects of drought on leaf physiology and tree growth spreading northwards. Such a tendency towards exacerbated moisture-sensitive growth and physiology could override positive effects of enhanced leaf intercellular CO_2 concentrations, possibly resulting in Europe-wide declines of forest carbon gain in the coming decades.

KEYWORDS
carbon isotopes, climate change, dendroecology, drought stress, European forests, latitudinal gradients, *Pinus*, *Quercus*, stomatal control, tree rings

1 | INTRODUCTION

Understanding the physiological mechanisms underlying variations in forest productivity is a key priority in global change research. Factors such as tree age, forest structure and management, nutrient availability and pollution influence the carbon budget of forested areas. During the last decades, however, climate change and increased atmospheric CO_2 ($_{atm}CO_2$) have greatly altered the productivity of European forests (Nabuurs et al., 2013). To explore these dynamics, research efforts have usually been confined to local ecosystems, with some representative woody species and their interactions examined at small spatial scales (but see e.g., Girardin et al., 2016; Pretzsch et al., 2014). This approach is hampered by site-dependent effects and limited significance of these environmental conditions. A comprehensive understanding of tree functioning is urgently needed across broad regions in order to assess the potential and limits of forest carbon uptake globally (Chown, Gaston, & Robinson, 2004). Through the analysis of meaningful functional traits (Violle, Reich, Pacala, Enquist, & Kattge, 2014), the interpretation of spatio-temporal patterns of forest growth variability can provide comprehensive insights into the environmental responses that may change the services of forests for carbon storage in forthcoming decades (Anderegg et al., 2016).

The mechanisms and processes influencing forest growth are extremely variable (Gibert, Gray, Westoby, Wright, & Falster, 2016). Despite this complexity, regionally coherent multispecies responses have been linked to global change effects on forest ecosystems using tree-ring networks. For example, Babst et al. (2013) found well-defined biogeographical patterns in climate response of forest growth across Europe following latitudinal/elevational gradients, and Shestakova et al. (2016) reported a *c*. 50% warming-induced enhanced growth synchrony in Iberian conifer forests during the 20th century. Indeed, dendroecological studies rely on the presence of common signals archived in tree populations, which are often derived from ring-width series reflecting variations of environmental factors (Fritts, 2001). Instead, stable isotopes are proxies of ecophysiological traits that are valuable to assess plant carbon and water relations at large spatio-temporal scales (Frank et al., 2015; Werner et al., 2012). In particular, the ratio of the heavy to light carbon isotopes ($^{13}C/^{12}C$) of organic matter depends on factors controlling the photosynthetic rate (A) and stomatal conductance (g_s) of the plant (Farquhar, Ehleringer, & Hubick, 1989). Given that the carbon isotope discrimination ($\Delta^{13}C$) of tree rings reflects more directly the complex array of tree responses to the environment than classical traits, such as ring width (Gessler et al., 2014; Treydte et al., 2007), the interannual variation in tree-ring $\Delta^{13}C$ is often used retrospectively to recover information on leaf-level physiological processes (e.g., Andreu-Hayles et al., 2011; Berninger, Sonninen, Aalto, & Lloyd, 2000; Shestakova, Aguilera, Ferrio, Gutiérrez, & Voltas, 2014). This is especially relevant in temperate forests thriving in near-optimal conditions, where tree growth fluctuations may not be as sensitive to climatic factors as stable isotopes (Hartl-Meier et al., 2015). Indeed, additional information can be gained by analysis of carbon isotopes in comparison to ring widths (Cernusak & English, 2015). Both proxies provide evidence on how trees respond to climate change and increasing $_{atm}CO_2$ (Andreu-Hayles et al., 2011; Saurer et al., 2014).

In drought-prone environments, tree-ring $\Delta^{13}C$ can be related mainly to the stomatal control of CO_2 fluxes, integrating environmental conditions affecting stomatal conductance (Gessler et al., 2014). In such conditions, radial growth (sink activity) and $\Delta^{13}C$ (source activity) are linked by two primary factors, stomatal regulation and water availability, with the feedback of sink activity on source activity being signalled through the phloem (Körner, 2015). However, radial growth and $\Delta^{13}C$ are progressively affected by changes in irradiance, temperature or nutritional stresses when water becomes less limited (Livingston et al., 1998; Rossi et al., 2016). By combining ring width and $\Delta^{13}C$, information on tree performance can be gained that underlies biogeographical interactions, because such traits share spatial responses to drought events (Voelker, Meinzer, Lachenbruch, Brooks, & Guyette, 2014).

In the present study, we attempt to investigate the degree of association between stem growth and photosynthetic carbon isotope fractionation across European forests using a unique tree-ring network. So far, only the isotope data of this network have been analysed (Treydte et al., 2007), but not radial growth, nor their relationships. In this regard, Treydte et al. (2007) reported strong similarities in the response of carbon and oxygen isotope records to summer moisture conditions, suggesting a tight link at the leaf level mediated through variation in stomatal conductance caused by the combined effect of varying temperature and precipitation conditions (Scheidegger et al., 2000). We used 20 chronologies assembled from old trees comprising conifers (mainly *Pinus*) and oaks (*Quercus*) spanning the 20th century and ranging from Mediterranean to boreal latitudes (37– 69°N). Indeed, latitudinal gradients are extremely relevant for the analysis of large-scale patterns of trait variability and their relationships with ecosystem functioning (Violle et al., 2014). We hypothesize that, on a continental scale: (a) temperature exerts (as a consequence of its large spatial homogeneity) a greater influence than drought on the spatial signals imprinted in tree rings; (b) the relationship between ring width and $\Delta^{13}C$ reflects the relative significance of carbon assimilation and stomatal regulation on tree performance, with positive relationships reflecting photosynthesis limited by stomatal conductance at low- and mid-latitude sites, and negative relationships suggesting temperature- or light-limited carbon uptake at high-latitude sites; and (c) widespread warming-induced drought stress triggers a tighter stomatal control of water loss that strengthens the relationship between growth and $\Delta^{13}C$ at low- and mid-latitude sites, as the stomatal sensitivity to drought becomes more limiting for carbon uptake. Therefore, we predict more synchronous growth linked to coordinated stomatal responses across species and regions as the climate becomes warmer and drier along the latitudinal gradient. On the basis of the combined analysis of radial growth and $\Delta^{13}C$, the assessment of spatio-temporal tree

responses to environmental changes may improve our knowledge of changes in growth and physiology experienced by European forests throughout the 20th century.

2 | MATERIALS AND METHODS

2.1 | Tree-ring network

We used a tree-ring dataset from the pan-European network ISONET (European Union, EVK2-2001-00237). It comprises 23 sites and provides a comprehensive coverage of the biogeographical conditions that are found across Europe into northern Africa (Treydte et al., 2007). The sites consist of old-growth forests (mean ± *SD* age = 454 ± 196 years) from the two main genera in Europe (*Pinus* and *Quercus*) plus *Cedrus atlantica* (Morocco) (Table 1). Three sites were discarded from the original network because they were located > 1,000 km apart from the nearest site (one site in southern Italy) or because they could not be assigned properly to a climate type consistent with that of nearby sites (two sites from high-elevation forests of the Alps) (for details, see subsection 2.4). The forests extend from cool dry summer (Mediterranean basin) to humid temperate (western-central Europe), cold continental (north-central Europe) and subarctic (Fennoscandia) climates (Table 1; Figure 1). The sampled trees are temperate oaks [*Quercus petraea* (three sites) and *Quercus robur* (five sites)] and Euro-Siberian pines [*Pinus nigra* (two sites), *Pinus sylvestris* (eight sites) and *Pinus uncinata* (one site)] plus *Cedrus atlantica* (one site), which has its phylogenetic origin in northern Eurasia (Qiao et al., 2007). Sampled stands show broad latitudinal (from 32°58 to 68°56' N) and elevational (from 5 to 2,100 m a.s.l.) gradients. High-elevation sites are concentrated in southern Europe. Mean annual temperature (MAT) varies between −1.2 and 11.5 °C among sites, with January being the coldest month (range −14.1 to 5.1 °C) and July the warmest month (11.9–19.6 °C). Mean annual precipitation (MAP) is highly variable, ranging from 432 to 1,517 mm across sites (Climatic Research Unit, CRU TS 3.21; Harris, Jones, Osborn, & Lister, 2014). Water deficit (i.e., evapotranspiration exceeding precipitation) occurs for 1 up to 7 months (from March to October) depending on the geographical location (Table 1). Conifers are the dominant species in boreal and Mediterranean zones (i.e., high-latitude or high-elevation sites), whereas oaks are mainly found in humid western and central European lowlands. The distance between sites varies from *c*. 50 to 4,500 km.

2.2 | Ring width and carbon isotope information

Increment cores were extracted from dominant trees (site mean = 46 trees; median = 28; Supporting Information Table S1), and tree-ring width (TRW) series were produced and cross-dated at the site level following standard dendrochronological procedures (Cook & Kairiukstis, 1990). The TRW was measured under a binocular microscope with precision of 0.01 mm. Visual cross-dating and ring-width measurements were validated using the program COFECHA (Holmes, 1983). Individual series were then subjected to detrending with the Friedman supersmoother spline with variable span tweeter sensitivity $\alpha = 5$ (Friedman, 1984) and posterior autoregressive modelling. This procedure aims to eliminate biological growth trends and potential disturbance effects and generates stationary series of dimensionless residual indices (TRW_i) that preserve a common interannual variance (i.e., high-frequency variability potentially related to climate). Finally, site chronologies (20) were obtained by averaging the indexed values of the series using a bi-weight robust mean (Cook & Kairiukstis, 1990). These procedures were performed using the program ARSTAN (Cook & Krusic, 2013). The quality of the resulting site chronologies was evaluated by calculation of the mean inter-series correlation (*Rbar*) and the expressed population signal (*EPS*) statistics. An *EPS* value of 0.85 was used to evaluate adequacy of the sample size for capturing a trustworthy population signal (Wigley, Briffa, & Jones, 1984). All chronologies were found to be well replicated during the 20th century (Supporting Information Table S1).

At least two accurately dated intact cores with clear ring boundaries and absence of missing rings from four or more trees per site were selected for subsequent carbon isotope analyses. Detailed information on sample preparation and α-cellulose extraction can be found in the paper by Treydte et al. (2007). In general, the whole ring was analysed for conifers, whereas only latewood was used for oaks. Treydte et al. (2007) reported that the type and magnitude of climate signals recorded in the isotopic network did not show obvious species-specific differences. To account for changes in $\delta^{13}C$ of atmospheric CO_2 ($\delta^{13}C_{air}$) attributable to fossil fuel combustion, carbon isotope discrimination ($\Delta^{13}C$) was estimated from $\delta^{13}C_{air}$ and α-cellulose $\delta^{13}C$ in plant material ($\delta^{13}C$), as described by Farquhar et al. (1989). Indexed $\Delta^{13}C$ chronologies ($\Delta^{13}C_i$) were obtained following the same procedure as described for ring width. Hence, any physiological long-term trend (e.g., decadal-scale variability driven by potential changes in the response of trees to increased CO_2; McCarroll et al., 2009; Treydte et al., 2009) was assumed to be removed from the series. In this way, we focused on the physiological basis of growth responses to high-frequency climate variability. The TRW_i and $\Delta^{13}C_i$ chronologies were used as input for statistical analyses. The study period was 1901–2003.

Additionally, basal area increment (BAI) was calculated as a proxy for above-ground woody biomass accumulation. For this purpose, individual ring-width series were converted into BAI records and detrended using the regional curve standardization (RCS) method (Briffa & Melvin, 2011). This approach aimed at eliminating age/size effects but preserving long-term growth changes driven by environmental conditions (Peters et al., 2015). Next, the residual indices of BAI series were averaged at the site level using a bi-weight robust mean. Temporal trends in the resultant BAI chronologies were estimated through the slope of the linear regression of BAI records over the 20th century, and significant trends were determined using the non-parametric Kendall τ rank correlation coefficient (Supporting Information Table S1).

TABLE 1 Geographical features and climatic characteristics of the sampling sites

No.	Country	Site name	Code	Species	Latitude (° N)	Longitude (° E)	Elevation (m)	MAT (°C)	MAP (mm)	PET (mm)	MAP < PET	BAI trend, b (cm^2/year)	Köppen classification
1	Finland	Kessi, Inari	INA	*Pinus sylvestris sylvestris*	68.93	28.42	150	−1.2	432	413	Apr–Aug	0.038	Dfc, subarctic
2	Finland	Sivak., Ilomantsi	ILO	*Pinus sylvestris*	62.98	31.27	200	2.2	573	515	Apr–Aug	0.152*	Dfc, subarctic
3	Norway	Gutuli	GUT	*Pinus sylvestris*	62.00	12.18	800	0.7	586	512	Apr–Aug	0.115	Dfc, subarctic
4	Finland	Bromarv	BRO	*Quercus robur*	60.00	23.08	5	4.9	568	562	Apr–Aug	0.004	Dfb, cold continental
5	UK	Lochwood	LOC	*Quercus robur*	55.27	−3.43	175	7.4	1,517	589	Jun	−0.032	Cfb, humid temperate
6	Lithuania	Panemunes Silas	PAN	*Pinus sylvestris*	54.88	23.97	45	6.6	634	672	Apr–Sep	0.320***	Dfb, cold continental
7	Poland	Suwalki	SUW	*Pinus sylvestris*	54.10	22.93	160	6.7	619	686	Apr–Sep	−0.010	Dfb, cold continental
8	UK	Woburn Abbey	WOB	*Quercus robur*	51.98	−0.59	50	9.5	709	724	Apr–Sep	0.046	Cfb, humid temperate
9	Germany	Dransfeld	DRA	*Quercus petraea*	51.50	9.78	320	7.7	723	677	Apr–Sep	0.163*	Cfb, humid temperate
10	UK	Windsor	WIN	*Pinus sylvestris*	51.41	−0.59	10	9.5	763	738	Apr–Sep	0.102	Cfb, humid temperate
11	Poland	Niepolomice, Gibiel	NIE1	*Quercus robur*	50.12	20.38	190	8.0	676	674	Apr–Aug	0.156*	Dfb, cold continental
12	Poland	Niepolomice, Gibiel	NIE2	*Pinus sylvestris*	50.12	20.38	190	8.0	676	674	Apr–Aug	0.250***	Dfb, cold continental
13	France	Fontainebleau	FON	*Quercus petraea*	48.38	2.67	100	11.5	608	861	Mar–Sep	−0.129	Cfb, humid temperate
14	France	Rennes	REN	*Quercus robur*	48.25	−1.70	100	11.1	733	786	Apr–Sep	−0.064	Cfb, humid temperate
15	Austria	Lainzer Tiergarte	LAI	*Quercus petraea*	48.18	16.20	300	9.6	654	792	Mar–Sep	−0.024	Cfb, humid temperate
16	Austria	Poellau	POE	*Pinus nigra*	47.95	16.06	500	8.3	815	762	Apr-Aug	−0.053	Cfb, humid temperate
17	Spain	Pinar de Lillo	LIL	*Pinus sylvestris*	43.07	−5.25	1,600	5.1	1505	688	Jul–Aug	0.069	Csb, Mediterranean
18	Spain	Massis de Pedraforca	PED	*Pinus uncinata*	42.23	1.70	2,100	3.9	1,299	692	Jul–Aug	−0.052	Csb, Mediterranean
19	Spain	Sierra de Cazorla	CAZ	*Pinus nigra*	37.80	−2.95	1,816	8.9	712	1,014	May–Sep	0.022	Csb, Mediterranean
20	Morocco	Col du Zad	COL	*Cedrus atlantica*	32.97	−5.07	2,200	10.4	717	1,163	Apr–Oct	−0.055	Csb, Mediterranean

Note: Sites are sorted latitudinally, from north (top) to south (bottom). Climate parameters were obtained based on CRU TS 3.21 data over the period 1901–2003 (see Materials and Methods for details). Climate types were estimated using the Köppen classification (Köppen & Geiger, 1936). The significance of BAI trends was assessed using the Kendall's τ non-parametric rank correlation coefficient (*$p < 0.05$; **$p < 0.01$; ***$p < 0.001$).

Abbreviations: BAI = basal area increment; MAP = mean annual precipitation; MAT = mean annual temperature; PET = potential evapotranspiration.

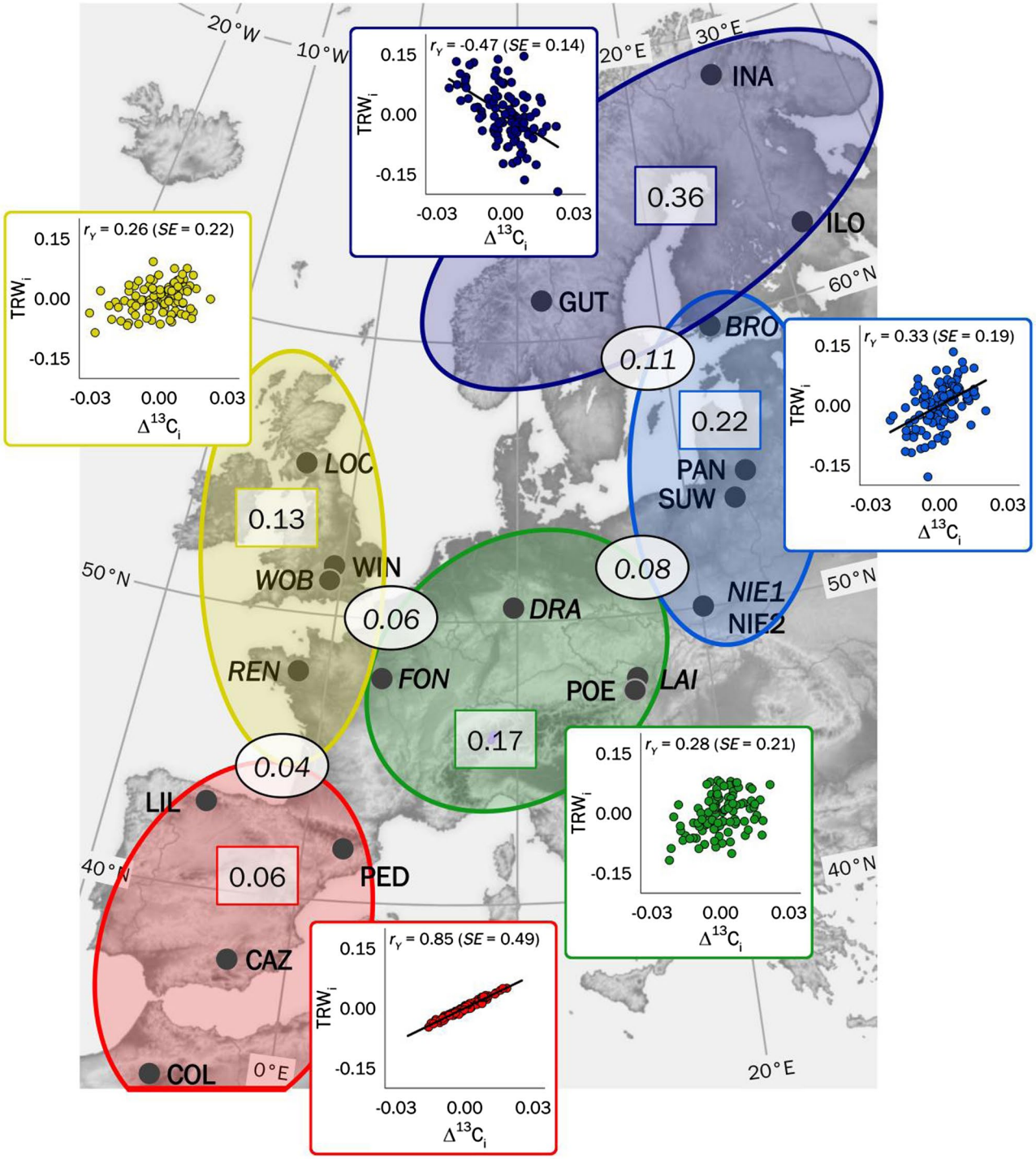

FIGURE 1 Geographical distribution of sites, definition of groups of chronologies, synchrony of radial growth ($\hat{a}$), and relationship between TRW$_i$ and $\Delta^{13}C_i$ chronologies (r_Y) at the group level across Europe. Each dot identifies a chronology composed of $n \geq 20$ trees according to the codes shown in Table 1 (oak codes are shown in italic). Each coloured encircled area identifies a group of chronologies that are separated in pairs up to 1,000 km apart and belong to a particular climate type as indicated in Table 1 (see Figure 2c for the distance threshold where significant radial growth patterns are shared among chronologies). At least three sites of the same climate type form a group (total number of groups, n = 5). Values of $\hat{a}$ and r_Y are estimated using indexed chronologies for the period 1901–2003 as described in the Supporting Information (Appendix S1.1). Growth synchrony ($\hat{a}$) is shown within a rectangle at the within-group level and within an ellipse at the between-group level. Only chronologies belonging to pairs of groups that are geographically close (i.e. neighbour groups) have between-group synchrony values statistically different from zero for the entire study period (as shown in the figure). The correlations at the group level (r_Y) are tested directly in a bivariate mixed model using restricted maximum likelihood (REML), and estimates are shown in the insets together with their standard error (*SE*). The scatterplots show year-level estimates (BLUPs) of TRW$_i$ and $\Delta^{13}C_i$ extracted from the bivariate model. Significant correlations (those having confidence intervals that do not straddle zero, 90% confidence interval approximated as $r_Y \pm 1.64SE$) are indicated with lines. The high *SE*s are partly explained by the errors of BLUP predictions that are carried forward in the bivariate analyses [Colour figure can be viewed at wileyonlinelibrary.com]

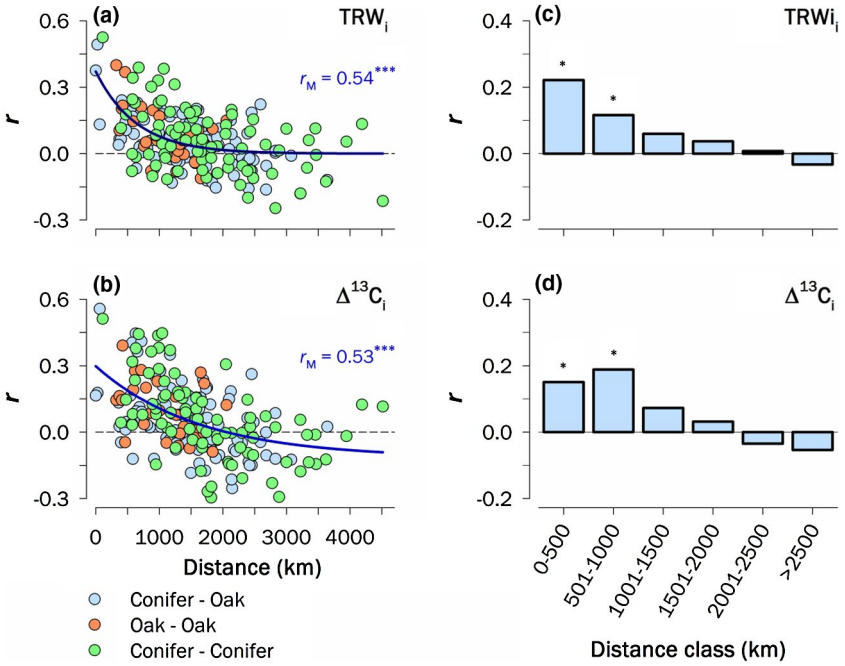

FIGURE 2 Spatial patterns of indexed tree-ring traits across Europe for the period 1901–2003: (a, c) indexed tree-ring width (TRW_i); and (b, d) indexed carbon isotope discrimination ($\Delta^{13}C_i$). Left panels show pairwise correlations of tree-ring chronologies as a function of geographical distance. The patterns are summarized by regressing the correlation coefficients (*r* values) involving pairs of chronologies (*y* axis) on their corresponding distance (*x* axis) by using negative exponential functions. Dot colours indicate pairwise correlations involving two conifer chronologies (green), two oak chronologies (orange), and one conifer and oak chronology (blue). Asterisks after the correlation coefficient (r_M) indicate the level of significance based on a Mantel test (***$p < 0.001$). Right panels show spatial structure of tree-ring traits across European forests. The spatial autocorrelation of the tree-ring network was characterized by six consecutive distance classes (listed on the *x* axis). Mean *r* values and their statistical significance (*p*) within each distance class were estimated from 1,000 randomizations. Significant correlation coefficients (*$p < 0.05$) are indicated [Colour figure can be viewed at wileyonlinelibrary.com]

2.3 | Meteorological data

Monthly mean temperature, precipitation and potential evapotranspiration (PET) were used for climate characterization. Meteorological variables were obtained from the nearest grid point of each site of the high-resolution climate dataset (Climatic Research Unit, CRU TS 3.21; Harris, Jones, Osborn, & Lister, 2014). The CRU provides climate series on a 0.5°×0.5° grid-box basis, interpolated from meteorological stations across the globe, and extends back to 1901. However, it should be noted that climate data mainly originate from low-elevation stations, and this leads to remarkable differences in elevation between stations and sampling sites in mountainous Mediterranean areas. To account for this discrepancy, we applied lapse rate adjustments to the CRU dataset for the Mediterranean sites (< 45° N), following Gandullo (1994). Potential evapotranspiration was estimated from CRU records using the Hargreaves method (Hargreaves & Samani, 1982).

Bootstrapped correlations between TRW_i or $\Delta^{13}C_i$ chronologies and monthly temperature, precipitation and the standardized precipitation–evapotranspiration index (SPEI3, a 3-month integrated drought index integrating evaporative demand and water availability; Vicente-Serrano, Beguería, & López-Moreno, 2010) were computed over the period 1901–2003 to examine site-specific responses to climate. We used SPEI3 because June–August is the period of highest climate responsiveness across the network for both TRW_i and, especially, $\Delta^{13}C_i$. To ensure that results were driven by local climate rather than by long-term trends (e.g., global warming), the climatic series exhibiting a linear trend over time were detrended by fitting a straight line and keeping the residuals of these linear fits or, otherwise, they were simply subtracted from the grand mean. Climate relationships were analysed from the previous October to the current September of tree-ring formation.

2.4 | Analysis of spatio-temporal patterns of tree-ring traits: methodological steps

The following steps were applied to characterize the nature and strength of common tree-ring patterns present in the network: (a) we described the spatial structure of indexed tree-ring traits (TRW_i and $\Delta^{13}C_i$) across Europe through correlogram analyses; (b) we investigated the temporal coherence of TRW_i among chronologies of the same or different climate type (i.e., within- and between-group, respectively) through variance–covariance (VCOV) modelling; and (c) we quantified the relationships between TRW_i and $\Delta^{13}C_i$ at the group level through a bivariate random model.

2.4.1 | Characterization of the spatial structure of tree-ring traits across Europe

The spatial structure of tree-ring traits was characterized for site pairs to determine how far common tree-ring patterns extend over Europe. This was done independently for TRW_i and $\Delta^{13}C_i$ as follows: (a) correlation coefficients (r) calculated between all possible pairs of site chronologies, calculated over the period 1901–2003, were regressed on their geographical distance using a negative exponential function; (b) the statistical significance of these pairwise correlations was assessed within distance classes located 500 km apart (a compromise between number of classes and statistical power) using the modified correlogram technique (Koenig & Knops, 1998). After (b), six classes were defined ranging from < 500 to > 2,500 km, with chronologies farther than 2,500 km apart combined into a single class. The same analyses were performed for MAT and MAP in order to evaluate the geographical extent of temporal coherence in such factors.

2.4.2 | Temporal coherence of tree-ring width

The investigation of TRW_i variability among chronologies (growth synchrony, $\hat{a}$) was performed through variance–covariance (VCOV) modelling following Shestakova et al. (2014, 2018) (Supporting Information Appendix S1.1). This approach tests for the presence of different tree-ring patterns for pre-established groups of chronologies, where particular groups can be defined based on existing knowledge (Shestakova et al., 2018). Here, the 20 chronologies were divided into four groups, classified according to particular climate types following the Köppen climate classification (Köppen & Geiger, 1936): boreal (Dfc), cold continental (Dfb), humid temperate (Cfb) and Mediterranean (Csb) (Table 1). Additionally, the humid temperate climate sites were split into Atlantic (for western Europe chronologies) and temperate (for central Europe chronologies) groups. These two groups resulted from a restriction of the maximum distance among sites belonging to the same group to 1,000 km (i.e., the spatial range of common tree-ring patterns continent-wide as inferred from correlograms). Therefore, five different groups were defined. Each group consisted of three to five neighbouring forest stands that ensured a solution to mixed model estimates.

A number of VCOV models accommodating between- and within-group variability were evaluated and compared using Akaike and Bayesian information criteria for model selection, which favour parsimonious models (Burnham & Anderson, 2002). The VCOV models were broad evaluation (constant variance across groups denoting a common growth pattern, or common synchrony, continent-wide), narrow evaluation (a banded main diagonal matrix denoting no common pattern or perfect asynchrony between groups), unstructured (a completely general covariance matrix indicating lack of systematic common patterns in the network), compound symmetry (a matrix having constant variance and covariance designating the same within-group pattern and the same between-group pattern) and variants of a Toeplitz structure [a matrix allowing for different (co) variances (denoting different patterns or synchrony values) according to the ordinal proximity or neighbourhood among groups]. These models are described in detail in Supporting Information Table S2. Estimates of growth synchrony ($\hat{a}$) were derived using the best VCOV model for the entire period (1901–2003) (Shestakova et al., 2018). In addition, the evolution of changes in $\hat{a}$ was studied for successive 50-year segments (i.e., half the study period) lagged 5 years by fitting the same VCOV models to each segment. This was done to characterize shifts in common TRW_i variability over time. In this case, the best-fitting model was independently selected for each segment to allow for changes in data structure over time.

Relationships between TRW_i and $\Delta^{13}C_i$ at the group level

The temporal (yearly) relationship between TRW_i and $\Delta^{13}C_i$ (hereafter, r_Y) was investigated at the group level through a bivariate random-effects model (Supporting Information Appendix S1.2) (Shestakova et al., 2017). Broadly speaking, this approach estimates the extent to which TRW_i and $\Delta^{13}C_i$, determined for the same set of chronologies, contain overlapping information as a result of plant processes related to carbon uptake and water use. Hence, the relevance of a physiological trait ($\Delta^{13}C_i$) potentially linked to regional forest growth is quantified by estimating how much of TRW_i variability across chronologies is associated with the variability of isotopic records. This quantification is relevant for studying the variable role of a physiological tracer for productivity across large areas. The bivariate analysis was performed for the entire period (1901–2003). We also evaluated the changes in r_Y between TRW_i and $\Delta^{13}C_i$ chronologies for successive 50-year segments lagged 5 years.

Finally, the changes in growth synchrony ($\hat{a}$) and in the relationship between TRW_i and $\Delta^{13}C_i$ (r_Y) were evaluated across groups as a function of biophysical variables through simple correlations. We used geographical information (latitude, longitude and elevation) and the following climatic records averaged across sites for every group (period 1901–2003): MAT, MAP and PET, following Hargreaves and Samani (1982). These relationships were assessed through correlation analysis for the complete period 1901–2003 and the split 1901–1950 and 1951–2003 periods.

3 | RESULTS

3.1 | Absolute growth trends and climate responses of indexed chronologies

Five sites showed positive BAI trends (slope b, $p < 0.05$) for the period 1901–2003, whereas no significant trend was detected for the remaining sites (Table 1). In particular, growth acceleration was observed at two oak sites and at three pine sites from mid and high latitudes of continental Europe. The analysis of climate responses revealed that high summer temperatures increased TRW_i in Fennoscandia principally (Supporting Information Figure S1a). Conversely, drought stress often constrained TRW_i at central and southern latitudes, as indicated by negative correlations with summer temperature and positive correlations with summer precipitation (Supporting Information

Figure S1a,b). Furthermore, strong ($r > 0.4$) positive correlations with SPEI3 that often extended from May to September denoted seasonal drought control of forest growth (Supporting Information Figure S1c). In addition, the positive TRW_i responses to high winter temperatures observed at some mid- and low-latitude sites suggested co-limitation by cold winters and dry summers. In comparison, more clear-cut, strong ($|r| > 0.4$) climate signals were detected continent-wide for $\Delta^{13}C_i$ records, which were influenced by summer temperatures (negatively), summer precipitation (positively) and, especially, summer SPEI3 (positively) (Supporting Information Figure S1d–f).

3.2 | Spatial consistency of tree-ring signals

The correlations between pairs of chronologies for TRW_i decreased with increasing distance between sites. This effect accounted for 29% of the variability of inter-site correlation coefficients if subject to exponential decay (Figure 2a). The highest correlations were found between *Quercus* stands from central Europe and between *Pinus* stands from north-eastern Europe ($r \geq 0.30$). For $\Delta^{13}C_i$, we also found an exponential decrease in common signal with distance for site pairs, which accounted for 28% of the variability of inter-site correlation coefficients (Figure 2b). Significant spatial autocorrelation was observed up to 1,000 km for TRW_i, with a mean correlation of 0.22 and 0.12 for sites within distances of 0–500 and 501–1,000 km, respectively (Figure 2c). Spatial autocorrelation was also found for $\Delta^{13}C_i$ up to 1,000 km (Figure 2d). A principal component analysis performed on TRW_i returned five principal components (PCs) that accounted for 50% of the total variance. The first PC, which explained 12.9% of variance, had positive loadings for all chronologies, except for one Iberian site with *P. sylvestris* and the Moroccan site with *C. atlantica* (Supporting Information Figure S2). The highest PC1 loadings corresponded to western and central European chronologies, indicating larger growth similarities compared with peripheral chronologies, located farther away from each other. The second PC, which explained 11.0% of variance, was also related to the geographical location of chronologies: positive PC2 loadings corresponded to south-western chronologies, whereas north-eastern chronologies had negative loadings (Supporting Information Figure S2). The remaining three PCs accounted for < 10% of variance and showed mixed spatial signals, indicating species-specific differences with the influence of local conditions on tree growth.

Likewise, the analysis of spatial autocorrelation of climate parameters revealed that the common signal declined with distance (Supporting Information Figure S3a,b) and extended > 2,500 km for MAT (linear function) and up to 1,000 km for MAP (decay function) (Supporting Information Figure S3c,d). There was also a significant negative relationship between the most distant sites (> 2,500 km) for MAP.

3.3 | Tree growth synchrony across Europe

The five climate groups identified for the network consisted of three to five chronologies sharing growth patterns (Figure 1). A heterogeneous Toeplitz structure with two bands was the best VCOV model for the period 1901–2003, indicating covariation between neighbouring groups only (Supporting Information Table S3). Growth synchrony ($\hat{a}$) varied considerably across groups, ranging from 0.06 ± 0.01 (Mediterranean) to 0.36 ± 0.06 (boreal) (mean ± *SE*) (Figure 1). The $\hat{a}$ values were unrelated to the average distance between sites at the group level, with groups showing the lowest and highest $\hat{a}$ having inter-site distances of 785 ± 118 and 913 ± 119 km (mean ± *SE*), respectively. The variable number of chronologies at the group level did not influence $\hat{a}$. At the between-group level, the highest $\hat{a}$ was found between boreal and cold continental forests (0.11 ± 0.02), with progressively decreasing common signals between group neighbours observed southwards (Figure 1). Differences in synchrony among groups were geographically structured and related to latitude ($r = 0.96$, $p < 0.01$) and longitude ($r = 0.89$, $p < 0.05$), but not to elevation (Supporting Information Figure S4).

To check for geographical consistency of synchrony gradients across Europe, we examined an independent, larger set of ring-width chronologies obtained from the International Tree-Ring Data Bank (Grissino-Mayer & Fritts, 1997) having the same species representation ($n = 80$; 52 *Pinus* chronologies and 28 *Quercus* chronologies). In this case, we also detected a strong latitudinal gradient in $\hat{a}$ ($r = 0.83$, $p < 0.05$). Consequently, we assumed that this trend was essentially independent of the particular tree-ring network examined. The observed geographical gradient in growth synchrony was also analysed in relationship to the potential climatic drivers of forest performance across Europe. Notably, climate variables explained most of the geographical variation in $\hat{a}$ among the five groups: strong negative relationships between $\hat{a}$ and PET ($r = -0.96$, $p < 0.01$), MAP ($r = -0.92$, $p < 0.05$) and MAT ($r = -0.81$, $p < 0.10$) were consistent with a gradual decrease in evapotranspirative demand, temperature and (elevation-driven) precipitation with increasing latitude.

3.4 | Temporal changes in growth synchrony

The synchrony patterns changed markedly across Europe over the 20th century. The value of $\hat{a}$ increased at low and mid latitudes (i.e., in Atlantic, Mediterranean and temperate forests), whereas it decreased at high latitudes (especially in boreal, but also in cold continental forests) (Figure 3a). Such divergent geographical trends modified the relationship between $\hat{a}$ and biogeographical factors, resulting in geographically gentler $\hat{a}$ gradients across the continent after 1950 (Supporting Information Figure S4). At the between-group level, different trends were observed depending on the combination of groups. For neighbouring groups, we found a substantial decrease in synchrony between boreal and cold continental forests, whereas synchrony remained steady or increased for other group combinations (Figure 3b). A modest, albeit sizeable common signal emerged among the more geographically distant group pairs after 1960 ($\hat{a}c$. 0.05–0.10) (Figure 3c). In fact, synchrony among forest types converged across Europe in the second half of the century. In contrast, we did not find changes in synchrony patterns of climate parameters (MAT and MAP) throughout the

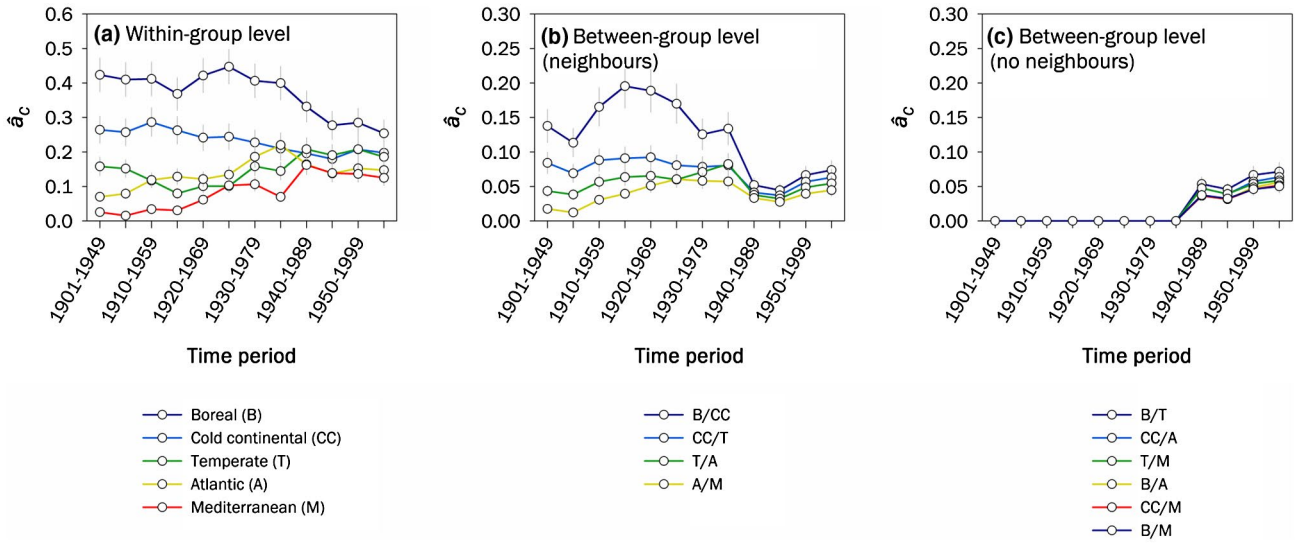

FIGURE 3 Temporal trends in growth synchrony at within- and between-group levels for the period 1901–2003. Growth synchrony ($\hat{a}$) is estimated for 50-year periods lagged by 5 years, following Equations 5 and 6 as described in the Supporting Information (Appendix S1.1). All calculations are based on indexed ring-width (TRW_i) chronologies. For the sake of visual clarity, the estimates of $\hat{a}$ are represented separately for chronologies belonging to the same group (i.e., within-group level; a), for chronologies belonging to pairs of groups that are geographically close (i.e. neighbour groups; b), and for chronologies belonging to pairs of groups that are geographically distant (c). Grey lines denote the *SE*. Note the change in scale of the *y* axis between panels [Colour figure can be viewed at wileyonlinelibrary.com]

20th century (results not shown). Therefore, the observed changes in growth synchrony could not have been driven by concomitant fluctuations in synchrony of climate factors.

3.5 | Tree growth patterns as related to isotopic signals

The temporal variability shared by TRW_i and $\Delta^{13}C_i$ (r_Y) was investigated at the group level. We found very different, geographically structured relationships. The association was mainly positive (for Atlantic, cold-continental and temperate forests) or very positive (for Mediterranean forests), being significantly negative for boreal forests (Figure 1), hence following a latitudinal gradient ($r = -0.96$, $p < 0.01$). Conversely, r_Y was non-significant for either longitude or elevation. In addition, r_Y was correlated with climate variables at the group level, with the strongest positive association being found for both PET ($r = 0.94$, $p < 0.05$) and MAP ($r = 0.82$, $p < 0.10$). An analysis across climate types involving all site chronologies of *Quercus* spp. confirmed that the positive relationship observed in Central Europe was taxa independent ($r_Y = 0.32$, $SE = 0.21$).

The association between TRW_i and $\Delta^{13}C_i$ changed markedly across Europe throughout the 20th century (Figure 4). The r_Y turned from negative to non-significant in boreal forests, and changed from non-significant to positive in cold-continental (recently), temperate and Mediterranean forests. As a result, TRW_i and $\Delta^{13}C_i$ mainly became positively related across Europe. The latitudinal pattern of r_Y was also stronger in the second half ($r = -0.95$, $p < 0.05$) than in the first half of the century ($r = -0.58$, n.s.). This relationship became more dependent on PET after 1950 ($r = 0.95$, $p < 0.05$) than before 1950 ($r = 0.68$, n.s.).

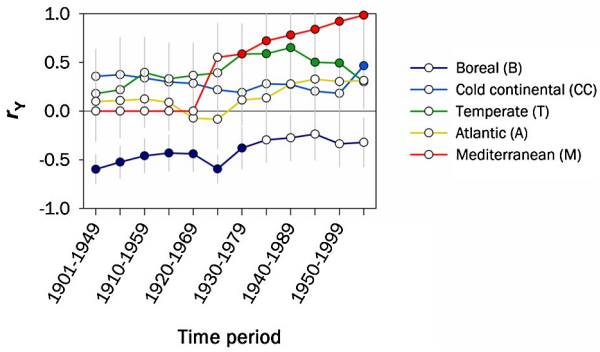

FIGURE 4 Temporal trends of relationships between TRW_i and $\Delta^{13}C_i$ chronologies at the group level for the period 1901–2003. The correlations (r_Y) are estimated for 50-year periods lagged 5 years, following Equation 7 as described in the Supporting Information (Appendix S1.2). All calculations are based on indexed ring-width (TRW_i) and carbon isotope ($\Delta^{13}C_i$) chronologies. Grey lines denote the *SE* of r_Y. Significant correlations (correlation coefficients with 90% confidence intervals not embracing zero) are depicted by filled dots [Colour figure can be viewed at wileyonlinelibrary.com]

4 | DISCUSSION

This study yields evidence for geographically structured patterns of forest growth and its associations with carbon isotope fractionation processes across Europe. Common tree growth and physiology are shared by stands that are ≤ 1,000 km apart from each other. This outcome provides the geographical extent to which climate factors influence tree performance continent-wide; indeed, no other

environmental driver is likely to act on the same spatial scale at the high-frequency domain (Fritts, 2001).

4.1 | Geographical structure of climatic controls of tree-ring signals in European forests

Differential growth responses to climate were evident across the network, with temperature-sensitive growth at northern latitudes, precipitation-sensitive growth at central-southern latitudes, and mixed signals in temperate and high-elevation European forests (Babst et al., 2013). Conversely, the extent of common summer climate signals present in carbon isotopes suggests a tight stomatal control of water losses and, indirectly, photosynthetic activity at peak season across most of Europe (Cullen, Adams, Anderson, & Grierson, 2008). These results suggest a partial decoupling between leaf- and stem-level processes (Jucker et al., 2017) as the result of different potentially contributory processes: (a) environmental constraints governing sink activity (i.e. meristematic growth) before affecting source activity (i.e., carbon uptake), particularly during drought or low temperatures (Körner et al. 2015); (b) temporal shifts between foliar dynamics and xylogenesis (Seftigen et al., 2018); and (c) changes in carbon allocation patterns with increasing temperature, which may vary between different biomes and functional groups (Way & Oren, 2010).

4.2 | Interpreting ring-width patterns continent-wide

Our results show a marked geographical organization of 20th century growth patterns across Europe. The most conspicuous changes in synchronous tree growth occur along a north–south gradient, with $\hat{a}$ increasing northwards concurrent with a thermal gradient of decreasing temperature and reduced evapotranspiration. This agrees with our hypothesis of more synchronous growth in cold-limited, high-latitude forests owing to the greater spatial homogeneity of temperature effects on tree growth in northern Europe (Düthorn, Schneider, Günther, Gläser, & Esper, 2016). This is in contrast to the geographically complex drought events occurring in central and southern Europe (Orlowsky & Seneviratne, 2014), hence resulting in substantially less synchronous growth occurring at large spatial scales (Shestakova et al., 2016). It should be noted that the mixture of sites with different species (oaks or pines) at the mid-latitude climate types may have intrinsically reduced the magnitude of synchronous growth in central Europe. Likewise, the inclusion of a cedar chronology might have constrained synchrony at the southernmost (Mediterranean) group, although *C. atlantica* has a stomatal behaviour similar to *P. nigra* (Froux et al., 2002). Species-specific climate responses are indeed relevant to delineate valid biogeographical patterns of tree performance, as shown Europe-wide (Babst et al., 2013). Perhaps owing to the limited density of our network, we could not clearly identify such differences (Supporting Information Figure S1), but the investigation of a denser dataset with nearly the same species representation confirmed such a broad latitudinal gradient (Supporting Information Figure S5). Thus, the results of a common sampling effort of limited representativeness compare well with records compiled from miscellaneous investigations having particular goals, geographical scopes and sampling strategies.

Notably, $\hat{a}$ increased after 1950 except in Fennoscandia, hence weakening the northward trend of enhanced synchrony observed during the preceding period. It suggests warming-induced climatic forcing spreading across central and southern Europe, irrespective of species and local site conditions (Supporting Information Figure S6). This exogenous factor enhances synchrony, probably as the outcome of common tree sensitivity to increased water stress. The results are in line with previous findings of high-frequency adjustments of ring-width patterns in response to amplified drought effects on growth in temperate and semi-arid regions (Latte, Lebourgeois, & Claessens, 2015; Shestakova et al., 2016). In contrast, climate warming could progressively mitigate low-temperature constraints on tree performance occurring in boreal forests (Düthorn et al., 2016). This leads to an increasing importance of local (stand-level) effects on tree growth over time, hence triggering regional asynchrony (Shestakova et al., 2019). We interpret these phenomena as a sign of increasing drought impacts on forest growth dynamics expanding northwards across Europe, which are concurrent with temperature trends across the study area (+0.15 to + 0.35 °C/decade between 1960 and 2015; European Environment Agency, 2016).

4.3 | Carbon isotope fractionation points to spatial patterns of forest growth in Europe

We also investigated leaf-level physiological mechanisms linked to geographically structured temporal growth variability by modelling the common temporal signal present in TRW_i and $\Delta^{13}C_i$ through bivariate random-effects analysis. This approach is appropriate for investigating common constraints on forest growth and leaf physiology acting over large (continental) climate gradients, because site-level impacts on tree-ring traits (e.g., differential management, competition, soil depth and fertility) are explicitly set aside in the analysis.

For the entire study period, the positive relationship between TRW_i and $\Delta^{13}C_i$ at low and mid latitudes indicates that leaf-level physiology and tree growth are commonly driven by water stress, to a greater or lesser extent, south of *c*. 60° N in Europe (Figure 1). Therefore, it suggests that stomatal limitation of carbon assimilation is imprinted in tree growth over most of the study area (including e.g., France, Austria, Germany and Poland) during the 20th century. This observation is seemingly independent of differences in stomatal behaviour between oaks and pines (Roman et al., 2015). Regardless of the different amplitude of $\Delta^{13}C$ fluctuations determined by isohydric and anisohydric strategies, the observed high-frequency signals share similar characteristics across taxa, as already reported by Treydte et al. (2007). Conversely, the negative relationship between TRW_i and $\Delta^{13}C_i$ in Fennoscandia indicates that photosynthesis and meristematic activity are constrained by low temperatures/sunshine hours (Gagen et al., 2011). At cool, moist sites, the main control over water-use efficiency is assimilation rate, which can be limited by either enzyme activity (photon flux) or enzyme production (leaf

temperature or nitrogen availability). These limitations would increase $\Delta^{13}C$ at the expense of decreased carbon uptake, which may reduce radial growth. Undoubtedly, our results must be weighed against the limited spatial density of the sampling network, but they allow the delineation of broad geographical trends that have so far been difficult to ascertain continent-wide, in part owing to the unsystematic and sparse nature of data collection (Saurer et al., 2014). Besides, the observed trends agree with previous studies performed across smaller areas showing strong positive TRW_i versus $\Delta^{13}C$ correlations for trees growing in water-limited conditions, but weak correlations at wetter and colder sites (del Castillo, Voltas, & Ferrio, 2015; Voelker et al., 2014).

4.4 | Strengthening of $\Delta^{13}C$–growth relationships in response to climate change

The relationship between tree growth and carbon isotope fractionation was not stable during the 20th century, with a general tendency towards increasing $\Delta^{13}C$–growth coupling across Europe. Alongside the increase in growth synchrony observed in the Atlantic, temperate and Mediterranean groups, a change from non-significant to positive correlations across most continental Europe suggests intensified drought impacts on tree physiology since the 1970s. Remarkably, present-day climatic influences on continent-wide tree growth are predominantly related to water conservation strategies, as reflected in cellulose $\Delta^{13}C$. In this regard, we found evidence of growth enhancement in the network (positive BAI trends), but only in five high- and mid-latitude stands (> 50° N) composed of either *Quercus* spp. or *P. sylvestris*. In these sites, the increasing trend could be produced by an increase in photosynthetic rates or in meristematic activity, which are likely to be driven by a combination of rising CO_2, temperature and surface radiation. In contrast, drought stress seems to override a positive effect of enhanced leaf intercellular CO_2 concentration in the remaining sites, and particularly < 50° N (e.g., the Mediterranean group, where the relation TRW_i versus $\Delta^{13}C$ has became strongly positive since 1970), resulting in no change in productivity (Andreu-Hayles et al., 2011). However, such warming-induced drought effects influencing stomatal regulation are insufficient to provoke the 20th century Europe-wide decrease of forest transpiration, as demonstrated for the same network (Frank et al., 2015). Alternative factors (e.g., lengthened growing seasons or increased leaf area) might counterbalance the impacts of leaf-level gas exchange processes on whole-tree physiology (Frank et al., 2015).

In Fennoscandia, the negative ring-width dependence on $\Delta^{13}C$ vanished after 1950. This suggests that an earlier photosynthetic limitation of growth or, alternatively, a reduced meristematic activity determining low carbon uptake (as driven by low temperatures, high cloudiness or both factors) attenuated in recent decades. In the western Mediterranean, this dependence changed abruptly from zero to nearly one after 1970. Previously, growth synchrony among the Mediterranean chronologies was absent, rendering a null signal shared by ring width and $\Delta^{13}C$. After 1950, the common growth signal was low but relevant; this signal was essentially related to $\Delta^{13}C$ fluctuations, resulting in a highly positive correlation (albeit with a high *SE*; Figure 1). This correlation may be interpreted in terms of a tight stomatal control of common radial growth in high-mountain Mediterranean forests, but it could also imply drought-driven reductions of sink activity controlling photosynthesis (Muller et al., 2011). However, the limited number of chronologies and the sudden change in tree performance during the 20th century might call these interpretations into question. A recent study carried out in Iberian mountain forests allows the downscaling of our results to a local area (Shestakova et al., 2017). These authors reported that multispecies tree growth at *c*. 1,500 m is more associated with a tighter stomatal control of water losses (inferred from $\Delta^{13}C$) since the 1980s, hence resembling lower-elevation stands. These results reinforce our view, although more data supporting this evidence are still needed on a regional scale. Unfortunately, studies on long-term shifts of radial growth related to switches of the main environmental drivers of photosynthetic carbon gain are still scarce (Voelker et al., 2014).

To conclude, we report on a shift in forest growth dependence from low temperatures to low moisture occurring southwards continent-wide and associated with latitudinal changes of tree carbon isotope fractionation processes. Leaf-level physiology and radial growth of trees are ultimately linked via carbon allocation strategies. Common signals imprinted in ring width and stable isotopes have been reported, either along geographical gradients (i.e., phenotypic plasticity; del Castillo et al., 2015), over time (i.e., temporal covariation; Voelker et al., 2014; Shestakova et al., 2017; this work) or at the intraspecific level (i.e., genetic correlation; Fardusi et al., 2016). These lines of evidence support (direct or indirect) effects of carbon uptake processes on above-ground growth. However, carbohydrates are used for various processes other than growth (e.g., maintenance, respiration, reproduction), and carbon availability might seldom limit tree growth (Palacio, Hoch, Sala, Körner, & Millard, 2014; but see Wiley & Helliker, 2012), which suggests that the relationship between productivity and stable isotopes might not be straightforward (Jucker et al., 2017). Alternative physiological mechanisms related to above-ground growth might interact with photosynthetic processes; for example, a critical turgor disrupting cell growth or the appearance of hydraulic constraints under drought (Sperry, 2000), or the weakening of meristematic growth under low temperatures (Rossi et al., 2016). These mechanisms would need to be assessed carefully against stable isotope signals.

Together with climate change, the increasing $_{atm}CO_2$ might have played a role in the observed shift in growth synchrony and the stronger relationship between $\Delta^{13}C$ and TRW_i. Disentangling the relative effects of climate and CO_2 fertilization on spatially structured tree-ring information is challenging because both low- and high-frequency signals influence the behaviour of tree physiology, carbon allocation and above- and below-ground growth. Additional factors interacting with climate change and $_{atm}CO_2$, such as increasing nutrient limitations (Jonard et al., 2015) or atmospheric deposition (de Vries, Dobbertin, Solberg, van Dobben, & Schaub, 2014), should also be

considered. A previous study on the same tree-ring network demonstrated that CO_2 fertilization has increased water-use efficiency of European forests in the 20th century (Saurer et al., 2014). However, these increments were not spatially uniform and, notably, the strongest increase was reported in response to summer drought for temperate forests in central Europe, an area in which we observe a large rise in growth–$\Delta^{13}C$ coupling. These findings point to an increase of water stress spreading northwards across Europe, which could result in declines of forest carbon gain in the coming decades. Therefore, broad-scale climatic variation influences tree ecophysiology and productivity in previously unrecognized ways and points to coordinated shifts in forest growth dynamics and a progressive convergence in the response of trees to the new climate conditions across Europe.

ACKNOWLEDGMENTS

T.A.S. acknowledges the ERANET-Mundus program (Euro-Russian Academic Network-Mundus, European Commission, grant agreement 20112573), the COST Action FP1304 (European Cooperation in Science and Technology) via the STSM program (Short-Term Scientific Missions, European Commission, COST-STSM-ECOST-STSM-FP1304-140915-066395) and the Spanish Government (grant number AGL2015-68274-C3-3-R). This study was supported by the EU project ISONET (European Isotope Network, EVK2-2001-00237). IDL has received financial support through the Postdoctoral Junior Leader Fellowship Programme from "la Caixa" Banking Foundations (LCF/BQ/LR18/11640004). We are also grateful to Carmela Miriam D'Alessandro, Nathalie Etien, Marie-Thérèse Guillemin and Werner Laumer for field and laboratory assistance.

DATA ACCESSIBILITY

The tree-ring data used in this study are available in the International Tree Ring Data Bank (ITRDB). The $\delta^{13}C$ records are available in supporting information of Treydte et al. (2007), grl23621-sup-0003-fs02.eps file.

ORCID


Tatiana A. Shestakova https://orcid.org/0000-0002-5605-0299

REFERENCES

Anderegg, W. R. L., Klein, T., Barlett, M., Sack, L., Pellegrini, A. F., Choat, B., & Jansen, S. (2016). Meta-analysis reveals that hydraulic traits explain cross-species patterns of drought-induced tree mortality across the globe. *Proceedings of the National Academy of Sciences USA*, *113*, 5024–5029. https://doi.org/10.1073/pnas.1525678113

Andreu-Hayles, L., Planells, O., Gutiérrez, E., Muntan, E., Helle, G., Anchukaitis, K. J., & Schleser, G. H. (2011). Long tree-ring chronologies reveal 20th century increases in water-use efficiency but no enhancement of tree growth at five Iberian pine forests. *Global Change Biology*, *17*, 2095–2112. https://doi.org/10.1111/j.1365-2486.2010.02373.x

Babst, F., Poulter, B., Trouet, V., Tan, K., Neuwirth, B., Wilson, R., … Frank, D. (2013). Site- and species-specific responses of forest growth to climate across the European continent. *Global Ecology and Biogeography*, *22*, 706–717. https://doi.org/10.1111/geb.12023

Berninger, F., Sonninen, E., Aalto, T., & Lloyd, J. (2000). Modeling ^{13}C discrimination in tree rings. *Global Biogeochemical Cycles*, *14*, 213–223.

Briffa, K. R., & Melvin, T. M. (2011). A closer look at regional curve standardization of tree-ring records: Justification of the need, a warning of some pitfalls, and suggested improvements of its application. In M. K. Hughes, H. F. Diaz, & T. W. Swetnam (Eds.), *Dendroclimatology: Progress and prospects* (pp. 113–145). Berlin: Springer Verlag.

Burnham, K. P., & Anderson, D. R. (2002). *Model selection and multi-model inference: A practical information-theoretic approach* (p. 488). New York: Springer.

Cernusak, L. A., & English, N. B. (2015). Beyond tree-ring widths: Stable isotopes sharpen the focus of climate response of temperate forest trees. *Tree Physiology*, *35*, 1–3.

Chown, S. L., Gaston, K. J., & Robinson, D. (2004). Macrophysiology: Large-scale patterns in physiological traits and their ecological implications. *Functional Ecology*, *18*, 159–167. https://doi.org/10.1111/j.0269-8463.2004.00825.x

Cook, E. R., & Kairiukstis, L. A. (1990). *Methods of dendrochronology: Applications in the environmental sciences*. Dordrecht, Netherlands: Springer, Netherlands.

Cook, E. R., & Krusic, P. J. (2013). *Program ARSTAN. A tree-ring standardization program based on detrending and autoregressive time series modeling, with interactive graphics*. Palisades, NY: Columbia University.

Cullen, L. E., Adams, M. A., Anderson, M. J., & Grierson, P. F. (2008). Analyses of $\delta^{13}C$ and $\delta^{18}O$ in tree rings of *Callitris columellaris* provide evidence of a change in stomatal control of photosynthesis in response to regional changes in climate. *Tree Physiology*, *28*, 1525–1533.

de Vries, W., Dobbertin, M. H., Solberg, H., van Dobben, H. F., & Schaub, M. (2014). Impacts of acid deposition, ozone exposure and weather conditions on forest ecosystems in Europe: An overview. *Plant and Soil*, *380*, 1–45. https://doi.org/10.1007/s11104-014-2056-2

del Castillo, J., Voltas, J., & Ferrio, J. P. (2015). Carbon isotope discrimination, radial growth, and NDVI share spatiotemporal responses to precipitation in Aleppo pine. *Trees*, *29*, 223–233. https://doi.org/10.1007/s00468-014-1106-y

Düthorn, E., Schneider, L., Günther, B., Gläser, S., & Esper, J. (2016). Ecological and climatological signals in tree-ring width and density chronologies along a latitudinal boreal transect. *Scandinavian Journal of Forest Research*, *31*, 750–757. https://doi.org/10.1080/02827581.2016.1181201

European Environment Agency. (2016). *Trends in annual temperature across Europe between 1960 and 2015*. Retrieved from http://www.eea.europa.eu/data-and-maps/figures/decadal-average-trends-in-mean-6

Fardusi, M. S., Ferrio, J. P., Comas, C., Voltas, J., Resco de Dios, V., & Serrano, L. (2016). Intra-specific association between carbon isotope composition and productivity in woody plants: A meta-analysis. *Plant Science*, *251*, 110–118. https://doi.org/10.1016/j.plantsci.2016.04.005

Farquhar, G. D., Ehleringer, J. R., & Hubick, K. T. (1989). Carbon isotope discrimination and photosynthesis. *Annual Review of Plant Physiology and Plant Molecular Biology*, *40*, 503–537. https://doi.org/10.1146/annurev.pp.40.060189.002443

Frank, D. C., Poulter, B., Saurer, M., Esper, J., Huntingford, C., Helle, G., … Weigl, M. (2015). Water-use efficiency and transpiration across European forests during the Anthropocene. *Nature Climate Change*, *5*, 579–584. https://doi.org/10.1038/nclimate2614

Friedman, J. H. (1984). *A variable span smoother*. Stanford, CA: Stanford University.

Fritts, H. C. (2001). *Tree rings and climate*. Caldwell, NJ: Blackburn Press.

Froux, F., Huc, R., Ducrey, M., & Dreyer, E. (2002). Xylem hydraulic efficiency versus vulnerability in seedlings of four contrasting

Mediterranean tree species (*Cedrus atlantica*, *Cupressus sempervirens*, *Pinus halepensis* and *Pinus nigra*). *Annals of Forest Science*, *59*, 409–418.

Gagen, M., Zorita, E., McCarroll, D., Young, G. H. F., Grudd, H., Jalkanen, R., … Kirchhefer, A. (2011). Cloud response to summer temperatures in Fennoscandia over the last thousand years. *Geophysical Research Letters*, *38*, L05701. https://doi.org/10.1029/2010GL046216

Gandullo, J. M. (1994). *Climatología y ciencia del suelo*. Madrid, Spain: Fundación Conde del Valle de Salazar.

Gessler, A., Ferrio, J. P., Hommel, R., Treydte, K., Werner, R., & Monson, R. K. (2014). Stable isotopes in tree rings: Toward a mechanistic understanding of fractionation and mixing processes from the leaves to the wood. *Tree Physiology*, *34*, 796–818.

Gibert, A., Gray, E. F., Westoby, M., Wright, I. J., & Falster, D. S. (2016). On the link between functional traits and growth rate: Meta-analysis shows effects change with plant size, as predicted. *Journal of Ecology*, *104*, 1488–1503. https://doi.org/10.1111/1365-2745.12594

Girardin, M. P., Bouriaud, O., Hogg, E. H., Kurz, W., Zimmermann, N. E., Metsaranta, J. M., … Bhatti, J. (2016). No growth stimulation of Canada's boreal forest under half-century of combined warming and CO_2 fertilization. *Proceedings of the National Academy of Sciences USA*, *113*, E8406–E8414.

Grissino-Mayer, H. D., & Fritts, H. C. (1997). The International Tree-Ring Data Bank: An enhanced global database serving the global scientific community. *Holocene*, *7*, 235–238. https://doi.org/10.1177/095968369700700212

Hargreaves, G. H., & Samani, Z. A. (1982). Estimating potential evapotranspiration. *Journal of the Irrigation & Drainage Division - ASCE*, *108*, 225–230.

Harris, I., Jones, P. D., Osborn, T. J., & Lister, D. H. (2014). Updated high-resolution grids of monthly climatic observations – the CRU TS3.10 Dataset. *International Journal of Climatology*, *34*, 623–642. https://doi.org/10.1002/joc.3711

Hartl-Meier, C., Zang, C., Büntgen, U., Esper, J., Rothe, A., Göttlein, A., … Treydte, K. (2015). Uniform climate sensitivity in tree-ring stable isotopes across species and sites in a mid-latitude temperate forest. *Tree Physiology*, *35*, 4–15. https://doi.org/10.1093/treephys/tpu096

Holmes, R. L. (1983). Computer-assisted quality control in tree-ring dating and measurement. *Tree Ring Bulletin*, *43*, 69–78.

Jonard, M., Fürst, A., Verstraeten, A., Thimonier, A., Timmermann, V., Potočić, N., … Rautio, P. (2015). Tree mineral nutrition is deteriorating in Europe. *Global Change Biology*, *21*, 418–430. https://doi.org/10.1111/gcb.12657

Jucker, T., Grossiord, C., Bonal, D., Bouriaud, O., Gessler, A., & Coomes, D. A. (2017). Detecting the fingerprint of drought across Europe's forests: Do carbon isotope ratios and stem growth rates tell similar stories? *Forest Ecosystems*, *4*, 24. https://doi.org/10.1186/s40663-017-0111-1

Koenig, W. D., & Knops, J. M. H. (1998). Testing for spatial autocorrelation in ecological studies. *Ecography*, *21*, 423–429. https://doi.org/10.1111/j.1600-0587.1998.tb00407.x

Köppen, W., & Geiger, R. (1936). *Handbuch der klimatologie*. Berlin, Germany: Gebrüder Bornträger.

Körner, C. (2015). Paradigm shift in plant growth control. *Current Opinion in Plant Biology*, *25*, 107–114. https://doi.org/10.1016/j.pbi.2015.05.003

Latte, N., Lebourgeois, F., & Claessens, H. (2015). Increased tree-growth synchronization of beech (*Fagus sylvatica* L.) in response to climate change in northwestern Europe. *Dendrochronologia*, *33*, 69–77. https://doi.org/10.1016/j.dendro.2015.01.002

Livingston, N. J., Whitehead, D., Kelliher, F. M., Wang, Y. P., Grace, J. C., Walcroft, A. S., … Millard, P. (1998). Nitrogen allocation and carbon isotope fractionation in relation to intercepted radiation and position in a young *Pinus radiata* D. Don tree. *Plant, Cell & Environment*, *21*, 795–803.

McCarroll, D., Gagen, M. H., Loader, N. J., Robertson, I., Anchukaitis, K. J., Los, S., … Waterhouse, J. S. (2009). Correction of tree ring stable carbon isotope chronologies for changes in the carbon dioxide content of the atmosphere. *Geochimica et Cosmochimica Acta*, *73*, 1539–1547. https://doi.org/10.1016/j.gca.2008.11.041

Muller, B., Pantin, F., Génard, M., Turc, O., Freixes, S., Piques, M., & Gibon, Y. (2011). Water deficits uncouple growth from photosynthesis, increase C content, and modify the relationships between C and growth in sink organs. *Journal of Experimental Botany*, *62*, 1715–1729. https://doi.org/10.1093/jxb/erq438

Nabuurs, G. J., Lindner, M., Verkerk, P. J., Gunia, K., Deda, P., Michalak, R., & Grassi, G. (2013). First signs of carbon sink saturation in European forest biomass. *Nature Climate Change*, *3*, 792–796. https://doi.org/10.1038/nclimate1853

Orlowsky, B., & Seneviratne, S. I. (2014). On the spatial representativeness of temporal dynamics at European weather stations. *International Journal of Climatology*, *34*, 3154–3160. https://doi.org/10.1002/joc.3903

Palacio, S., Hoch, G., Sala, A., Körner, C., & Millard, P. (2014). Does carbon storage limit tree growth? *New Phytologist*, *201*, 1096–1100. https://doi.org/10.1111/nph.12602

Peters, R. L., Groenendijk, P., Vlam, M., & Zuidema, P. A. (2015). Detecting long-term growth trends using tree rings: A critical evaluation of methods. *Global Change Biology*, *21*, 2040–2054. https://doi.org/10.1111/gcb.12826

Pretzsch, H., Biber, P., Schütze, G., Uhl, E., & Rötzer, T. (2014). Forest stand growth dynamics in Central Europe have accelerated since 1870. *Nature Communications*, *5*, 4967. https://doi.org/10.1038/ncomms5967

Qiao, C.-Y., Ran, J.-H., Li, Y., & Wang, X.-Q. (2007). Phylogeny and biogeography of *Cedrus* (Pinaceae) inferred from sequences of seven paternal chloroplast and maternal mitochondrial DNA regions. *Annals of Botany*, *100*, 573–580. https://doi.org/10.1093/aob/mcm134

Roman, D. T., Novick, K. A., Brzostek, E. R., Dragoni, D., Rahman, F., & Phillips, R. P. (2015). The role of isohydric and anisohydric species in determining ecosystem-scale response to severe drought. *Oecologia*, *179*, 641–654. https://doi.org/10.1007/s00442-015-3380-9

Rossi, S., Anfodillo, T., Čufar, K., Cuny, H. E., Deslauriers, A., Fonti, P., … Treml, V. (2016). Pattern of xylem phenology in conifers of cold forest ecosystems at the Northern Hemisphere. *Global Change Biology*, *22*, 3804–3813.

Saurer, M., Spahni, R., Frank, D. C., Joos, F., Leuenberger, M., Loader, N. J., … Young, G. H. (2014). Spatial variability and temporal trends in water-use efficiency of European forest. *Global Change Biology*, *20*, 332–336.

Scheidegger, Y., Saurer, M., Bahn, M., & Siegwolf, R. (2000). Linking stable oxygen and carbon isotopes with stomatal conductance and photosynthetic capacity: A conceptual model. *Oecologia*, *125*, 350–357. https://doi.org/10.1007/s004420000466

Seftigen, K., Frank, D. C., Björklund, J., Babst, F., & Poulter, B. (2018). The climatic drivers of normalized difference vegetation index and tree-ring-based estimates of forest productivity are spatially coherent but temporally decoupled in Northern Hemispheric forests. *Global Ecology and Biogeography*, *27*, 1352–1365. https://doi.org/10.1111/geb.12802

Shestakova, T. A., Aguilera, M., Ferrio, J. P., Gutiérrez, E., & Voltas, J. (2014). Unravelling spatiotemporal tree-ring signals in Mediterranean oaks: A variance–covariance modelling approach of carbon and oxygen isotope ratios. *Tree Physiology*, *34*, 819–838. https://doi.org/10.1093/treephys/tpu037

Shestakova, T. A., Camarero, J. J., Ferrio, J. P., Knorre, A. A., Gutiérrez, E., & Voltas, J. (2017). Increasing drought effects on five European pines modulate Δ^{13}C-growth coupling along a Mediterranean altitudinal gradient. *Functional Ecology*, *31*, 1359–1370.

Shestakova, T. A., Gutiérrez, E., Kirdyanov, A. V., Camarero, J. J., Génova, M., Knorre, A. A., … Voltas, J. (2016). Forests synchronize their growth in contrasting Eurasian regions in response to climate warming. *Proceedings of the National Academy of Sciences USA*, *113*, 662–667. https://doi.org/10.1073/pnas.1514717113

Shestakova, T. A., Gutiérrez, E., Valeriano, C., Lapshina, E., & Voltas, J. (2019). Recent loss of sensitivity to summer temperature constrains tree growth synchrony among boreal Eurasian forests. *Agricultural and Forest Meteorology*, *268*, 318–330. https://doi.org/10.1016/j.agrformet.2019.01.039

Shestakova, T. A., Gutiérrez, E., & Voltas, J. (2018). A roadmap to disentangling ecogeographical patterns of spatial synchrony in dendrosciences. *Trees*, *32*, 359–370. https://doi.org/10.1007/s00468-017-1653-0

Sperry, J. S. (2000). Hydraulic constraints on plant gas exchange. *Agricultural and Forest Meteorology*, *104*, 13–23. https://doi.org/10.1016/S0168-1923(00)00144-1

Treydte, K., Frank, D. C., Esper, J., Andreu, L., Bednarz, Z., Berninger, F., … Schleser, G. H. (2007). Signal strength and climate calibration of a European tree-ring isotope network. *Geophysical Research Letters*, *34*, L24302. https://doi.org/10.1029/2007GL031106

Treydte, K., Frank, D. C., Saurer, M., Helle, G., Schleser, G. H., & Esper, J. (2009). Impact of climate and CO_2 on a millennium-long tree-ring carbon isotope record. *Geochimica et Cosmochimica Acta*, *73*, 4635–4647. https://doi.org/10.1016/j.gca.2009.05.057

Vicente-Serrano, S. M., Beguería, S., & López-Moreno, J. I. (2010). A multiscalar drought index sensitive to global warming: The Standardized Precipitation Evapotranspiration Index. *Journal of Climate*, *23*, 1696–1718. https://doi.org/10.1175/2009JCLI2909.1

Violle, C., Reich, P. B., Pacala, S. W., Enquist, B. J., & Kattge, J. (2014). The emergence and promise of functional biogeography. *Proceedings of the National Academy of Sciences USA*, *111*, 13690–13696. https://doi.org/10.1073/pnas.1415442111

Voelker, S. L., Meinzer, F. C., Lachenbruch, B., Brooks, J. R., & Guyette, R. P. (2014). Drivers of radial growth and carbon isotope discrimination of bur oak (*Quercus macrocarpa* Michx.) across continental gradients in precipitation, vapour pressure deficit and irradiance. *Plant, Cell and Environment*, *37*, 766–779.

Way, D. A., & Oren, R. (2010). Differential responses to changes in growth temperature between trees from different functional groups and biomes: A review and synthesis of data. *Tree Physiology*, *30*, 669–688. https://doi.org/10.1093/treephys/tpq015

Werner, C., Schnyder, H., Cuntz, M., Keitel, C., Zeeman, M. J., Dawson, T. E., … Gessler, A. (2012). Progress and challenges in using stable isotopes to trace plant carbon and water relations across scales. *Biogeosciences*, *9*, 3083–3111. https://doi.org/10.5194/bg-9-3083-2012

Wigley, T. M. L., Briffa, K. R., & Jones, P. D. (1984). On the average value of correlated time series, with applications in dendroclimatology and hydrometerology. *Journal of Applied Meteorology and Climatology*, *23*, 201–213.

Wiley, E., & Helliker, B. (2012). A re-evaluation of carbon storage in trees lends greater support for carbon limitation to growth. *New Physiologist*, *195*, 285–289. https://doi.org/10.1111/j.1469-8137.2012.04180.x

BIOSKETCH

Tatiana A. Shestakova is a postdoctoral researcher at the Woods Hole Research Center, Falmouth, MA, USA. Her research interests include dendroecology, stable isotope biogeochemistry and climate change impacts on the natural forest ecosystem. In particular, she works on designing efficient inference tools and algorithms based on mixed modelling principles to understand the processes underlying the complexity and diversity in tree response patterns to environmental forcing and how these patterns are spatially structured across biogeographical gradients.

SUPPORTING INFORMATION

Additional supporting information may be found online in the Supporting Information section at the end of the article.

How to cite this article: Shestakova TA, Voltas J, Saurer M, et al. Spatio-temporal patterns of tree growth as related to carbon isotope fractionation in European forests under changing climate. *Global Ecol Biogeogr*. 2019;28:1295–1309. https://doi.org/10.1111/geb.12933